



Characterizing the bio-functionalization of gold surface with total internal reflection fluorescence (TIRF) microscopy

Robin Ehrminger^a, Sergei Kopanchuk^b, Kairi Kivirand^{a,b}, Tavo Romann^b, Toonika Rincken^b,
Mart Min^a, and Ago Rincken^{b*}

^a Thomas Johann Seebeck Department of Electronics, Tallinn Technical University, Ehitajate tee 5, 19086 Tallinn, Estonia

^b Institute of Chemistry, University of Tartu, Ravila 14a, 50411 Tartu, Estonia

Received 20 May 2019, accepted 13 June 2019, available online 24 January 2020

© 2020 Authors. This is an Open Access article distributed under the terms and conditions of the Creative Commons Attribution-NonCommercial 4.0 International License (<http://creativecommons.org/licenses/by-nc/4.0/>).

Abstract. Quality of bioactive surface is crucial for achieving the required sensitivity and selectivity of biosensing systems. Numerous methods are available for the characterization of metal-coated surfaces, but only a few to test the efficacy of biomaterial immobilization and the level of non-specific binding. Herewith we propose to use total internal reflection fluorescence (TIRF) microscopy for the characterization of the surface analyte recognition capacity. Biomolecules were bound onto titanium/gold covered glass using three different self-assembled monolayers (SAM). The surfaces with attached antibodies were evaluated using the specific binding of fluorophore-labeled secondary antibodies and visualized with TIRF. Among studied SAMs, aminothiols layers with glutaraldehyde coupling demonstrated high binding capacity along with excellent homogeneity indicating their suitability for applications in biosensors.

Key words: TIRF microscopy, self-assembled monolayers, homogeneity, electrode surfaces, biosensing system, gold thin film.

1. INTRODUCTION

Biosensors are analytical tools, where biorecognition is used to detect analytes and convert obtained signals into measurable physical parameters. The ability of the biological element for specific interaction with the analyte of interest secures the selectivity of the determination. So, one of the main challenges in bioanalytical applications is to quantify and increase the capacity of the functional biorecognition components and avoid nonspecific interactions on the surface of electrodes.

Self-assembled monolayers (SAMs) can be used for the biofunctionalization and immobilization of bioactive materials onto electrodes. In addition to their binding properties, their hydrophobic nature minimizes non-specific binding. The quality of SAM layers and efficacy of surface immobilization has been studied extensively in different

systems as the level of selectivity, sensitivity, and assay robustness are crucial factors in biosensor applications. Atomic force microscopy (AFM) [1–4], cyclic voltammetry (CV) [5,6], electrochemical impedance spectroscopy (EIS) [7], quartz crystal microbalance (QCM) [8], surface plasmon resonance (SPR) [9–11], ellipsometry [12,13], X-ray photoelectron spectroscopy (XPS) [13,14], scanning electron microscope (SEM) [15,16], Raman microscopy [1], and scanning tunneling microscope (STM) [17] have been used for the characterization of SAM layers. Still, these methods do not provide direct information about the efficacy and quality of the immobilization of specific biological capturing elements and analyte recognition capacity of the surface.

In recent years several novel methods of fluorescence microscopy offer higher sensitivity and resolution to visualize different objects. Among them, total internal reflection fluorescence (TIRF) microscopy allows selective illumination of fluorophores in the very close

* Corresponding author, ago.rincken@ut.ee

proximity to the surface without illuminating fluorophores further in the solution, resulting in high contrast with single molecule detection capabilities [18]. For the detection of surface-bound fluorophores at the glass-water interface, the beam has to be excited at an oblique angle to generate the evanescent field and total internal reflection to allow the beam to propagate inside the coverslip [19]. TIRF microscopy can be used for the detection of binding capacity and homogeneity of surface-immobilized fluorophore-labeled biomolecules, e.g. antibodies [20] or enzymes [21]. TIRF microscopy can also be performed in combination with the metal enhanced surface plasmon-coupled emission (SPCE) to improve the contrast between the emission of the fluorophore and the background without quenching the fluorophore [22–24]. This means that it allows characterizing immobilized surfaces of thin metal layers as well. Herewith we propose to use SPCE enhanced TIRF microscopy as an optical method for the characterization of surfaces of biofunctionalized gold thin films electrodes. This approach enables direct access to surface-bound biomolecules with enhanced contrast to improve the quality of biofunctionalized electrodes utilized in the fields of SPR, QCM, CV, and EIS.

2. MATERIALS AND METHODS

2.1. Chemicals, solutions, and reagents

16-mercaptohexadecanoic acid (16-MHA, 90%), 6-amino-1-hexanethiol hydrochloride (6-AH), N-hydroxysuccinimide (NHS) were obtained from Sigma-Aldrich, 11-amino-1-undecanethiol hydrochloride (11-AU, $\geq 90.0\%$) was purchased from Dojindo, 1-ethyl-3-[3-dimethylaminopropyl] carbodiimide (EDC, $\geq 98\%$) from Alfa Aesar, glutaraldehyde (GA, 50% solution in water) from AppliChem, ethanolamine from Fisher Chemicals and goat polyclonal anti-rabbit IgG labelled with Alexa Fluor[®] 488 from Abcam (ab150077). Rabbit IgG antibodies were purified in the University of Tartu, Institute of Chemistry from rabbit antisera using protein A column (HiTrap[™] Protein A HP, 5 mL, GE Healthcare) and stored in 10 mM phosphate buffer saline (PBS with 0.15 M NaCl, pH 7.2) [25]. 16-MHA, 6-AH, and 11-AU were dissolved in ethanol (96%). Milli-Q water (18 M Ω /cm) was used for the preparation of solutions. All chemicals were of analytical grade and were used as received without further purification. The Schott glasses D 263[®] bio (No. 1.5 H and 22 × 22 mm) were purchased from Paul Marienfeld GmbH.

2.2. Magnetron sputtering of thin films

AJA International UHV (ultra-high vacuum) magnetron sputtering system was used to deposit titanium (Ti) and gold (Au) films at room temperature. The 1.5 nm Ti film

(adhesion layer) was deposited on a glass sample using 3” Ti (AJA International 99.999% purity) target, 3 mTorr Ar pressure, 300 W DC (direct current) power, and deposition time was 13 s. In the following step, 35 nm of Au film was deposited using 2” Au (AJA International 99.99% purity) target, 3 mTorr Ar pressure, 55 W PDC (pulsed direct current, 100 kHz frequency, 3-microsecond pulse) power at the sample, and deposition time was 3 min 32 s. According to ellipsometry measurements (GES-5E from “Semilab Co”, microspot option, incidence angle 70 deg), the thickness of the Au film was from 35 to 38 nm.

2.3. Preparation of the bio-functionalized electrodes

Figure 1 illustrates the preparation of biofunctionalized electrodes, starting with microscope coverslips directly after the sputtering process. The Ti/Au covered coverslips were incubated in surface modifying reagent for 24 hours in the dark at room temperature. The used solutions of modifiers were the following: 1 mM 6-AH (pH \approx 11) or 1 mM 11-AU (pH \approx 11) or 1 mM 16-MHA (pH \approx 2), all in ethanol. After the formation of SAM layers, the electrodes were rinsed with ethanol and Milli-Q water. Next, the 6-AH and 11-AU surfaces were incubated in 12.5% glutaraldehyde for 60 min. The surfaces with 16-MHA layers were incubated in a solution containing 0.1 M NHS and 0.4 M EDC for 30 min at room temperature to activate the terminal carboxylic groups. For the antibody attachment, the surfaces were incubated with 90 μ g/mL rabbit IgG antibody solution in 500 mM carbonate buffer (pH 9.5) (6-AH and 11-AU) or in 10 mM acetate buffer pH 5.0 (16-MHA) at 4 °C overnight and then rinsed with Milli-Q water. After covalent immobilization of antibodies, the surfaces were incubated with a solution of 1 M ethanolamine (pH 8.5) in Milli-Q water for 10 min at the room temperature to deactivate the remaining active functional groups. For the preparation of surfaces used for the detection of non-specific binding, all active functional groups of SAM layers were directly deactivated with ethanolamine. Finally, the surfaces were rinsed with 10 mM PBS buffer (0.15 M NaCl, pH 7.4) and stored in the same buffer at 4 °C for further usage.

2.4. Total internal reflection fluorescence (TIRF) set-up and measurements

The iXON897 (Andor) was mounted to the side port of an iMIC TIRF inverted digital fluorescence microscope (Till Photonics GmbH, Gräfelfing, Germany) through a TuCam adapter with 2× magnification (Andor Technology, Belfast, UK). For the illumination, the laser diode 488 nm from Omicron laser combiner was fibre-coupled to the Yanus Scan head and Polytrope for the regulation of the illumination angle. For the detection, the Olympus 60x APON NA 1.49 TIRF objective was used. The filter cube comprised of a

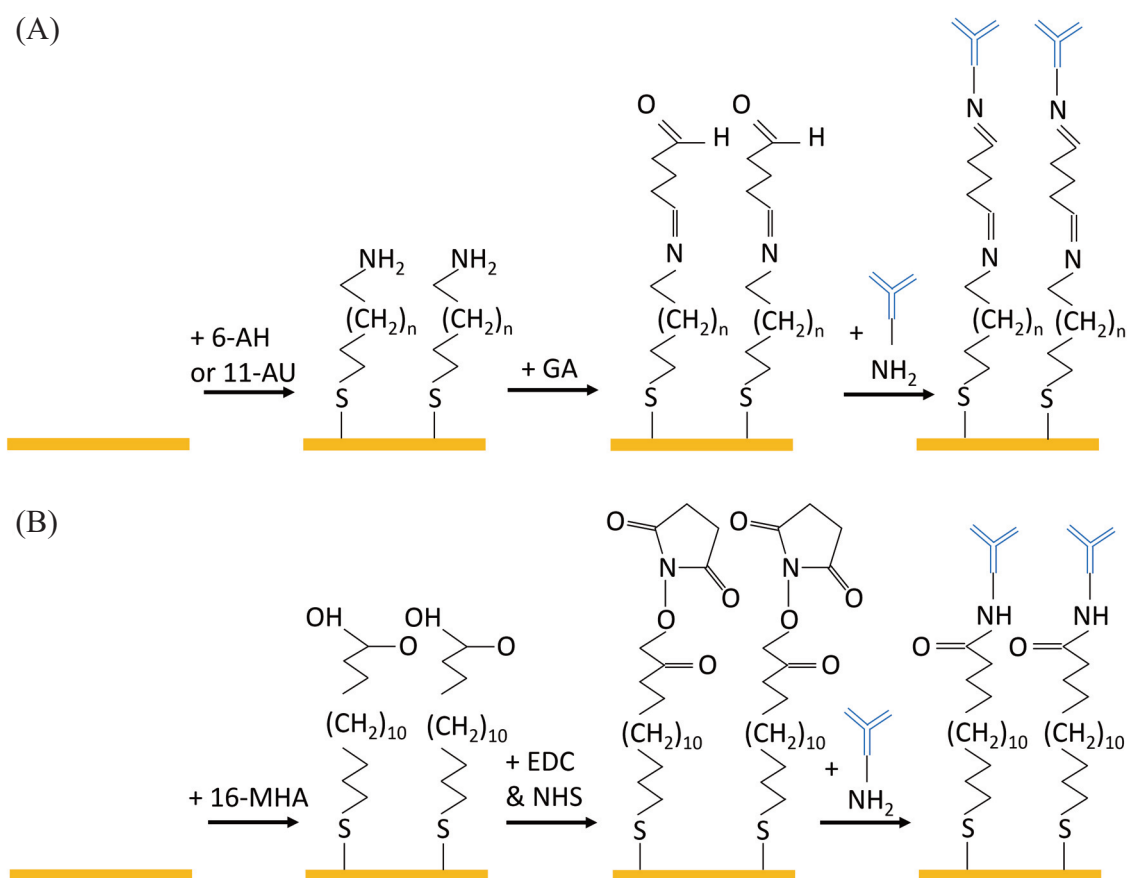


Fig. 1. Biofunctionalization of gold surfaces with rabbit IgG antibodies using different hydrophobic spacers: 6-amino-1-hexanethiol hydrochloride (6-AH) or 11-amino-1-undecanethiol hydrochloride (11-AU) (A) and 16-mercaptohexadecanoic acid (16-MHA) (B).

475/35 nm BrightLine HC exciter (Semrock, New York, USA), a zt 491 RDCXT dichroic beamsplitter (Chroma, Bellows Falls, USA), and a 525/45 nm BrightLine HC emitter (Semrock, New York, USA). Measurements were conducted on biofunctionalized coverslips mounted into magnetic CMS chambers (Live Cell Instruments, Korea). 10 nM Alexa 488 labelled anti-rabbit IgG antibody in Dulbecco's phosphate buffer saline (DPBS, pH 7.2) without Ca and Mg (ID 17-512, Lonza, Switzerland) was used for the detection of immobilized antibodies. The immobilized surfaces were incubated with the detecting antibody at room temperature for 20 min before each measurement. For all experiments, the same illumination power, illumination TIR angle, and exposure time were applied.

3. RESULTS AND DISCUSSION

The development of biofunctionalized electrodes for applications in the field of biosensing has common challenges like the capacity and reproducibility of selective binding sites and the homogeneity of their planar

distribution on the surface. The TIRF microscope together with metal enhanced surface plasmon-coupled emission opens new possibilities in this field.

In this study, the thin metal films consist of 1.5 nm Ti (adhesion layer) and 35 nm Au, which are deposited onto flat glass coverslips. These slides provide efficient transfer of light energy through the thin film as well as high electrical conductivity towards electrochemical biosensor systems. Comparing gold covered and uncovered slips we detected the enhancement of the detected TIRF signal and changing the incident angle of illumination along with the increase of Michelson contrast index in case of gold covered slides, which indicates the occurrence of SPCE component of this detection system.

The bulk properties of the base substrates (borosilicate microscopy coverslips made of Schott D 263[®] bio) were analysed with high-resolution SEM (Fig. 2) and AFM (Fig. 3) to characterize the flatness and, the non-porous texture of the microscopy coverslips before and after the deposition of thin films without biofunctional modifications.

These surface topography studies showed a flat surface with the RMS (root means square) roughness of

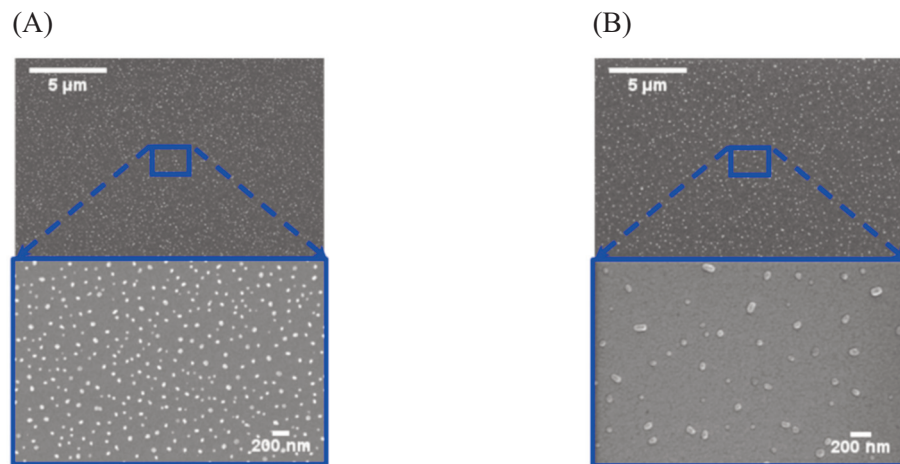


Fig. 2. High-resolution SEM microscopy image of the blank coverslip before (A) and after (B) the thin film deposition of 1.5 nm Ti (adhesion layer) and 35 nm Au using HR-SEM Zeiss Merlin equipped with an In-Lens SE detector for topographic imaging and In-Lens energy selective backscattered detector for compositional contrast. Measurements were taken at the operating voltage of 2 kV.

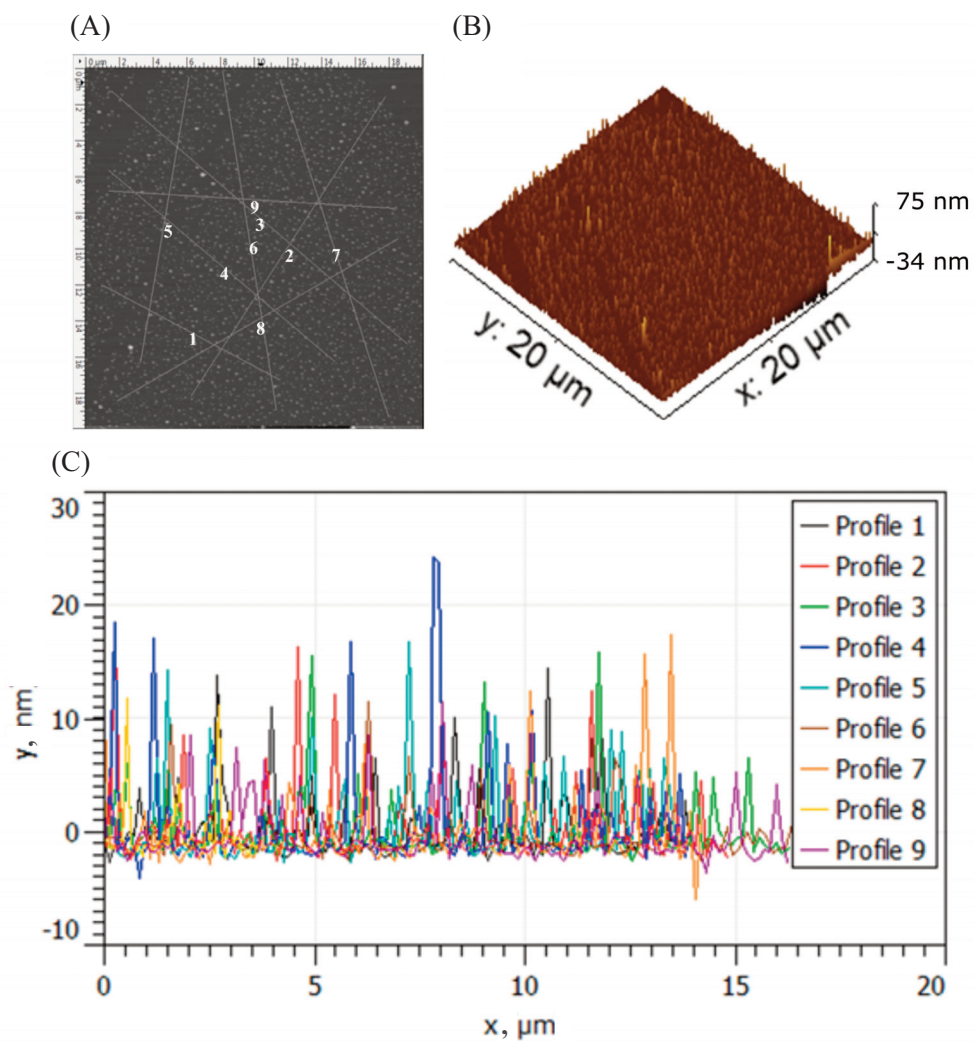


Fig. 3. The topology of the microscopy coverslip (Schott D 263[®] bio) surface after the magnetron sputtering to generate Ti/Au film. The AFM measurements were performed in non-contact mode with the Bruker NEOS 8 equipped with the reflex coating cantilever. The surface topology in 2D (A) and 3D (B) format is shown by a 20 × 20 μm frame with the representative profile of the surface (C).

2.1–2.3 nm and sparsely distributed peaks with heights between 14–25 nm. The high-resolution SEM images are pointing to a non-porous surface texture before and after the metal thin film deposition process, indicating that the metal layer partly covers inhomogeneity of the structures of the glass surface. AFM and high-resolution SEM reveal that the surface roughness, as well as the non-porous texture before and after the deposition of the thin metal films, can be considered for TIRF microscopy as non-significant. The smooth and non-porous texture is considered as particularly crucial for biosensor systems' applications as the topography directly influences the homogeneity, specific and non-specific binding capacity as well as the reproducibility of biofunctionalized electrodes. To bind bioactive components to the sensor and to avoid non-specific binding to the electrode, the thin films have to be covered by the SAM layer.

In this study, three commonly used SAM layers [26–28], all making use of the covalent S-H bridge on freshly deposited gold surfaces, were applied to bind bioselective components and avoid non-specific absorption of an analyte

to thin gold films. The bioactive component, rabbit IgG antibodies were covalently coupled to the SAM layer, and the quality of the bioactive layer on electrodes was assessed by specific binding of 10 nM Alexa 488-labeled anti-rabbit antibody. The detection of non-specific absorption of the secondary detecting antibody was performed in the absence of the capturing antibody on the SAM layers.

The first SAM layer investigated, was composed by the long-chain 16-mercaptohexadecanoic acid (16-MHA), which was biofunctionalized by immobilizing rabbit antibodies with the help of NHS and EDC via the amino groups of the antibody. The other SAM layers were produced with two different omega-amino-alkanethiols: 6-amino-1-hexanethiol hydrochloride (6-AH) and 11-amino-1-undecanethiol hydrochloride (11-AU) and the antibodies were attached to the amino groups of these alkanethiols with the help of glutaraldehyde (GA).

The results related to the specific and non-specific binding capacity and planar distribution of specific (and nonspecific) binding sites were detected in the form of

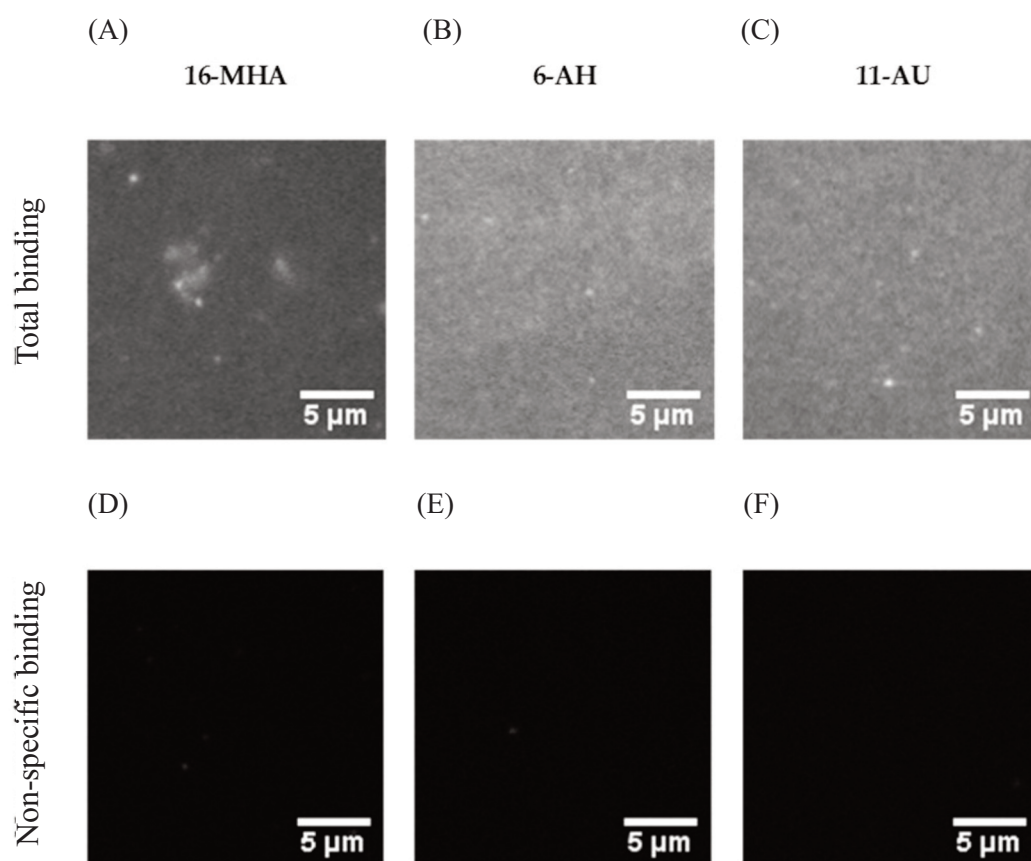


Fig. 4. TIRF images of Alexa 488-labelled anti-rabbit antibody binding to different electrodes. The biofunctionalized SAM layers were formed with 16-MHA (A, D), 6-AH (B, E) or 11-AU (C, F) and the spatial distribution of the total binding was measured in the presence of the capturing rabbit antibody (A-C), while the non-specific binding was detected in the absence of the capturing rabbit antibody (D-F). All TIRF images were taken in the presence of 10 nM anti-rabbit antibody labelled with Alexa 488 after 20 min incubation at room temperature.

Table 1. Intensity values and quality factors of different biofunctionalized SAM layers

SAM layer	Mean intensity value, arbitrary number $\times 10^3$ ^a	Level of non-specific binding, % ^b	Z-factor ^b
A 16-MHA	7.2 ± 1.0	7.6	0.57 ± 0.07
B 6-AH	11.3 ± 0.9	7.7	0.72 ± 0.02
C 11-AU	12.6 ± 0.9	5.4	0.76 ± 0.04

^a n = 10; measurements from 10 random fields of view of one biofunctionalized coverslip

^b n = 30; frames from the coverslips of three independent preparations, where measurements were done at 10 random fields of view per one coverslip.

intensity values of the TIRF images (Fig. 4 and Table 1). All SAM layers with attached antibodies provided strong specific interactions with lower than 10% of non-specific binding due to their hydrophobicity.

For the estimation of assay suitability for biosensing applications, we used a simple statistical parameter Z-factor for high throughput screening of the surfaces [29]. The Z-factor takes into account the means and standard deviations of both the positive and negative controls of the assay.

In our case, the Z-factor was derived from the standard deviation and mean intensity values of 16-bit greyscale TIRF microscopy images with the field of view of $20 \times 20 \mu\text{m}$. The data variability reflects the homogeneity of total and non-specific binding surfaces and, the magnitude of the response (mean intensity) that relates to the capacity of specific and non-specific binding. The obtained Z-factors (Table 1) indicated a good or excellent assay for all three SAM layers, although the distinctive differences between the different activation processes can be pointed out. The omega-amino-alkane thiols indicated higher homogeneity and higher binding activities compared to commonly used 16-mercaptohexadecanoic acid (16-MHA).

To compare the non-specific binding of the secondary detecting antibody to the different SAM layers in the absence of the capturing antibody, we produced TIRF images within a different range of contrast (Fig. 5). This allowed identifying apparent differences in the non-specific binding on different surfaces, which were hidden during the detection of total binding (Fig. 4D–F). Here we see that the general nonspecific binding decreases with the increase of the length of the hydrocarbon chain of the SAM layer. Even small defects detected do not interfere with the total low level of non-specific binding achieved.

To conclude, TIRF microscopy provides unique insights into the capacity of active binding sites, hydrophobic properties, and the homogeneity of distribution of both specific and non-specific binding sites in close proximity of a thin metal film. The results obtained suggest that TIRF microscopy with metal enhanced SPCE provides a highly sensitive platform for the investigation of the specific and non-specific binding capacity of activated SAM layers on metallic films. The proposed method allows the development and study of novel biofunctionalized layers for metal electrodes of biosensors using glass-based slides, where the quality of the bioactivated surfaces can be evaluated with TIRF and SPCE.

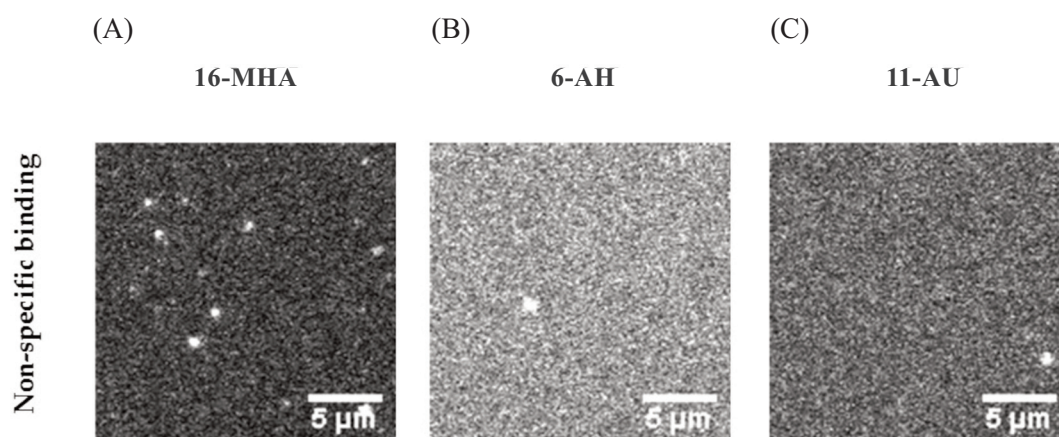


Fig. 5. TIRF images of non-specific binding of Alexa 488-labeled anti-rabbit antibody to electrodes with different SAM layers in the absence of the capturing antibody. The SAM layers were formed with 16-MHA (A), 6-AH (B) or 11-AU (C). The TIRF images were taken in the presence of 10 nM anti-rabbit antibody labeled with Alexa 488 and presented with increased contrast in the low-intensity range. The arbitrary intensity values were $(0.5 \pm 0.1) \times 10^3$ (A); $(0.8 \pm 0.2) \times 10^3$ (B) and $(0.6 \pm 0.1) \times 10^3$ (C).

ACKNOWLEDGMENTS

This research was funded by the Centre of Excellence in Information Technology (EXCITE); Estonian Research Council grants IUT 20-17, IUT 19-11 and PSG 230; grant 4.01.15-0011 of the European Regional Development Fund for the financing period 2014–2020; and grant SPS985291 from NATO. Our special thanks to Olga Volobujeva for the SEM measurements (Department of Material and Environmental Technology: Laboratory of Optoelectronic Materials Physics, Tallinn Technical University); and to Natalja Sleptšuk for the AFM studies (Thomas Johann Seebeck Department of Electronics: Research Laboratory for Cognitronics, Tallinn Technical University); and also to Aarne Kasikov for the thickness measurements performed by ellipsometry (Institute of Physics, University of Tartu). The publication costs of this article were covered by the Estonian Academy of Sciences.

REFERENCES

- Xue, Y., Li, X., Li, H., and Zhang, W. Quantifying thiol-gold interactions towards the efficient strength control. *Nat. Commun.*, 2014, **5**, 1–9. <https://doi.org/10.1038/ncomms5348>
- Lio, A., Charych, D. H., and Salmeron, M. Comparative Atomic Force Microscopy Study of the Chain Length Dependence of Frictional Properties of Alkanethiols on Gold and Alkylsilanes on Mica. *J. Phys. Chem. B*, 1997, **101**(19), 3800–3805. <https://doi.org/10.1021/jp963918e>
- Hegner, M., Wagner, P., and Semenza, G. Immobilizing DNA on gold via thiol modification for atomic force microscopy imaging in buffer solutions. *FEBS Lett.*, 1993, **336**(3), 452–456. [https://doi.org/10.1016/0014-5793\(93\)80854-N](https://doi.org/10.1016/0014-5793(93)80854-N)
- Marti, O., Colchero, J., and Mlynek, J. Combined scanning force and friction microscopy of mica. *Nanotechnology*, 1990, **1**(2), 141–144. <https://doi.org/10.1088/0957-4484/1/2/003>
- Shein, J. B., Lai, L. M. H., Eggers, P. K., Paddon-Row, M. N., and Gooding, J. J. Formation of Efficient Electron Transfer Pathways by Adsorbing Gold Nanoparticles to Self-Assembled Monolayer Modified Electrodes. *Langmuir*, 2009, **25**(18), 11121–11128. <https://doi.org/10.1021/la901421m>
- Eckermann, A. L., Feld, D. J., Shaw, J. A., and Meade, T. J. Electrochemistry of redox-active self-assembled monolayers. *Coord. Chem. Rev.*, 2010, **254**(15–16), 1769–1802. <https://doi.org/10.1016/j.ccr.2009.12.023>
- Radke, S. M. and Alocilja, E. C. A high density microelectrode array biosensor for detection of *E. coli* O157:H7. *Biosens. Bioelectron.*, 2005, **20**(8), 1662–1667. <https://doi.org/10.1016/j.bios.2004.07.021>
- Briand, E., Gu, C., Boujday, S., Salmann, M., Herry, J. M., and Pradier, C. M. Functionalisation of gold surfaces with thiolate SAMs: Topography/bioactivity relationship – A combined FT-RAIRS, AFM and QCM investigation. *Surf. Sci.*, 2007, **601**(18), 3850–3855. <https://doi.org/10.1016/J.SUSC.2007.04.102>
- Zamfir, L.-G., Geana, I., Bourigau, S., Rotariu, L., Bala, C., Errachid, A., et al. Highly sensitive label-free immunosensor for ochratoxin. A based on functionalized magnetic nanoparticles and EIS/SPR detection. *Sens. Actuators, B*, 2011, **159**(1), 178–184. <https://doi.org/10.1016/j.snb.2011.06.069>
- Peterson, A. W., Halter, M., Tona, A., Bhadriraju, K., and Plant, A. L. Surface plasmon resonance imaging of cells and surface-associated fibronectin. *BMC Cell Biol.*, 2009, **10**(16), 1–17. <https://doi.org/10.1186/1471-2121-10-16>
- Löfås, S., Johnsson, B., Edström, Å., Hansson, A., Lindquist, G., Müller-Hillgren, R.-M., et al. Methods for site controlled coupling to carboxymethyl-dextran surfaces in surface plasmon resonance sensors. *Biosens. Bioelectron.*, 1995, **10**(9–10), 813–822. [https://doi.org/10.1016/0956-5663\(95\)99220-F](https://doi.org/10.1016/0956-5663(95)99220-F)
- Porter, M. D., Bright, T. B., Allara, D. L., and Chidsey, C. E. D. Spontaneously organized molecular assemblies. 4. Structural characterization of n-alkyl thiol monolayers on gold by optical ellipsometry, infrared spectroscopy, and electrochemistry. *J. Am. Chem. Soc.*, 1987, **109**(12), 3559–3568. <https://doi.org/10.1021/ja00246a011>
- Troughton, E. B., Bain, C. D., Whitesides, G. M., Nuzzo, R. G., Allara, D. L., and Porter, M. D. Monolayer films prepared by the spontaneous self-assembly of symmetrical and unsymmetrical dialkyl sulfides from solution onto gold substrates: structure, properties, and reactivity of constituent functional groups. *Langmuir*, 1988, **4**(2), 365–385. <https://doi.org/10.1021/la00080a021>
- Parviz, M., Gaus, K., and Gooding, J. J. Simultaneous impedance spectroscopy and fluorescence microscopy for the real-time monitoring of the response of cells to drugs. *Chem. Sci.*, 2017, **8**(3), 1831–1840. <https://doi.org/10.1039/c6sc05159f>
- Techane, S. D., Gamble, L. J., and Castner, D. G. Multi-technique Characterization of Self-Assembled Carboxylic Acid-Terminated Alkanethiol Monolayers on Nanoparticle and Flat Gold Surfaces. *J. Phys. Chem. C*, 2011, **115**(19), 9432–9441. <https://doi.org/10.1021/jp201213g>
- Benmouna, R., Racht, V., Le Barny, P., Feneyrou, P., Maschke, U., and Coqueret, X. Polymer Dispersed Liquid Crystals with Nanosized Droplets: SEM, FTIR and UV Spectroscopy Studies. *J. Polym. Eng.*, 2006, **26**(7), 655–669. <https://doi.org/10.1515/POLYENG.2006.26.7.655>
- Koslowski, B., Tschetschetkin, A., Maurer, N., and Ziemann, P. 4-Mercaptopyridine on Au(111): a scanning tunneling microscopy and spectroscopy study. *Phys. Chem. Chem. Phys.*, 2011, **13**(9), 4045–4050. <https://doi.org/10.1039/c0cp02162h>
- Axelrod, D. Cell-substrate contacts illuminated by total internal reflection fluorescence. *J. Cell Biol.*, 1981, **89**(1), 141–145. <https://doi.org/10.1083/jcb.89.1.141>
- Axelrod, D. Selective imaging of surface fluorescence with very high aperture microscope objectives. *J. Biomed. Opt.*, 2001, **6**(1). <https://doi.org/10.1117/1.1335689>
- Jain, A., Liu, R., Xiang, Y. K., and Ha, T. Single-molecule pull-down for studying protein interactions. *Nat. Protoc.*, 2012, **7**(3), 445–452. <https://doi.org/10.1038/nprot.2011.452>
- Claessen, V. I., Engelkamp, H., Christianen, P. C. M., Maan, J. C., Nolte, R. J. M., Blank, K., and Rovan, A. E. Single-biomolecule kinetics: the art of studying a single enzyme. *Annu. Rev. Anal. Chem.*, 2010, **3**, 319–340. <https://doi.org/10.1146/annurev.anchem.111808.073638>
- Gryczynski, I., Malicka, J., Gryczynski, Z., and Lakowicz, J. R. Surface Plasmon-Coupled Emission with Gold

- Films. *J. Phys. Chem. B*, 2004, **108**(33), 12568–12574. <https://doi.org/10.1021/jp040221h>
23. Chizhik, A. I., Rother, J., Gregor, I., Janshoff, A., and Enderlein, J. Metal-induced energy transfer for live cell nanoscopy. *Nat. Photonics*, 2014, **8**, 124–127. <https://doi.org/10.1038/nphoton.2013.345>
 24. Lakowicz, J. R. *Principles of fluorescence spectroscopy*, 3rd ed. Springer, Boston, MA, 2006.
 25. Mikhlepp, K., Kivirand, K., Nikopensus, M., Peedel, D., Utt, M., and Rinken, T. Design and production of antibodies for the detection of *Streptococcus uberis*. *Enzyme Microb. Technol.*, 2017, **96**, 135–142. <https://doi.org/10.1016/j.enzmictec.2016.10.009>
 26. Kamińska, A., Witkowska, E., Winkler, K., Dzięcielwski, I., Weyher, J. L., and Waluk, J. Detection of Hepatitis B virus antigen from human blood: SERS immunoassay in a microfluidic system. *Biosens. Bioelectron.*, 2015, **66**, 461–467. <https://doi.org/10.1016/j.bios.2014.10.082>
 27. Im, H., Huang, X.-J., Gu, B., and Choi, Y.-K. A dielectric-modulated field-effect transistor for biosensing. *Nat. Nanotechnol.*, 2007, **2**(7), 430–434. <https://doi.org/10.1038/nnano.2007.180>
 28. Mirsky, V. M., Riepl, M., and Wolfbeis, O. S. Capacitive monitoring of protein immobilization and antigen–antibody reactions on monomolecular alkythiol films on gold electrodes. *Biosens. Bioelectron.*, 1997, **12**(9–10), 977–989. [https://doi.org/10.1016/S0956-5663\(97\)00053-5](https://doi.org/10.1016/S0956-5663(97)00053-5)
 29. Zhang, J.-H., Chung, T. D. Y., and Oldenburg, K. R. A Simple Statistical Parameter for Use in Evaluation and Validation of High Throughput Screening Assays. *J. Biomol. Screen.*, 1999, **4**(2), 67–73. <https://doi.org/10.1177/10870571990040206>

Biofunktsionaliseeritud kullapindade iseloomustamine täieliku sisepeegelduse fluorestsentsmikroskoopiaga

Robin Ehrminger, Sergei Kopanchuk, Kairi Kivirand, Tavo Romann, Toonika Rinken, Mart Min ja Ago Rinken

Biosensorsüsteemide arenduses on bioselektiivsete pindade valmistamisel nende reprodutseeritavuse kõrval väga oluline ka nende homogeensus. Kuigi metallipindade iseloomustamiseks on olemas mitmeid meetodeid, siis biomaterjali pinnale immobiliseerimise efektiivsuse ja erinevate ainete mittespetsiifilise seostumise suuruse kohta annavad infot ainult üksikud neist. Käesolevas töös kasutati täieliku sisepeegelduse fluorestsentsmikroskoopi, et iseloomustada analüüdi äratundmisreaktsioone kuldpinna kinnitatud biomolekulide poolt. Biomolekulide, milleks käesolevas töös olid antikehad, immobiliseerimiseks kuldpinna kasutati erinevaid sidumisstrateegiaid ja kinnitunud antikehade aktiivsust ning selektiivsust hinnati fluorofooriga märgistatud sekundaarsete antikehade seostumise järgi, mida jälgiti täieliku sisepeegelduse fluorestsentsmikroskoobi abil. Uuritud pindadest osutusid parimateks ω -aminoalküülthioolidega töödeldud pinnad, millele biomolekulid seoti glutaaraldehüüdiga. Nende pindade homogeensus, madal mittespetsiifiline sidumine ja suur sidumiskohtade arv teeb need süsteemid perspektiivseks erinevate biosensorsüsteemide arendamiseks.